RESEARCH ARTICLE

Adsorption and Thermodynamic Parameters of Activated Carbon-Diazepam Systems in Simulated Gastric Fluid

Carlos A. Ray-Mafull[1], Dachamir Hotza[2], Raquel García-Gallardo[3], Orlando F. Cruz Junior[4], Jarosław Serafin[5,6,*]

[1]Instituto de Ciencia y Tecnología de Materiales (IMRE-UH), Ciudad de la Habana, Cuba
[2]Universidade Federal de Santa Catarina (UFSC) Florianópolis, SC, Brazil
[3]Laboratorio Farmacéutico Reinaldo Gutiérrez, Ciudad de la Habana, Cuba
[4]Instituto Nacional de Pesquisas da Amazônia (INPA), Manaus, AM, Brazil
[5]Institute of Energy Technologies and Barcelona Research Center in Multiscale Science and Engineering, Universitat Politècnica de Catalunya. Eduard Maristany 16, EEBE, 08019 Barcelona, Spain
[6]Department of Chemical Engineering, Universitat Politècnica de Catalunya, Eduard Maristany 16, EEBE, 08019 Barcelona, Spain

*Corresponding author: E-mail: jaroslaw.serafin@upc.edu; Tel.: (+48) 697 058 192

DOI: 10.5185/amlett.2021.061637

In this study, the adsorption and thermodynamic parameters of Diazepam drugs adsorbed onto six activated carbons were determined. A simulated gastric fluid was applied at pH 1.2 for 4 h. The samples were characterized by FTIR, N_2 isotherm at 77 K, and CO_2 at 273 K. The experimental adsorption was fitted by isotherm models: Langmuir Type I and II, DR, Halsey, Freundlich, Harkins-Jura, Temkin, and BET. UV visible spectra monitored residual drugs. The results showed relationships between temperature increase, adsorbent characteristics, and the behavior of these drugs in acid solution. The positive values of all the isosteric adsorption enthalpies determined from the slope Van't Hoff plot (R^2>97) indicated the endothermic nature of the adsorption process. In all cases, $\Delta G<0$ so that the spontaneous character of the adsorption process was attested. Moreover, the positive values of ΔS stated that the randomness increased at the solid-solution interface during the adsorption process.

Introduction

In recent decades, activated carbon has been use satisfactorily in patients with drug poisoning. Since it is not absorbed by the digestive-tract, it absorbs a wide variety of chemical compounds and drugs. In addition to the ability of activated carbon to prevent oral absorption of drugs, oral administration of activated carbon has also been reported to increase the removal of many drugs [**1-4**]. The chemical structure of the adsorbate and the surface of the adsorbent are factors of interaction between the basal planes (nonspecific interaction) and the polar functional groups of the surface (specific interaction) [**5-8**].

The chemical structure of activated carbon associated with high surface area, pore size distribution and surface chemistry, provide an ideal material for the adsorption of organic compounds [**9-12**]. Decrease in free energy and entropy in the system accompany the adsorption process naturally. Kinetic effect, solubility, pH, temperature, chemical structure of the organic compound, surface area of the adsorbent are elements that can contribute to the adsorption process. The mechanisms that involve the surface interaction can be highlighted and explained by studying the thermodynamic parameters present in the adsorption process [**13-18**]. The aim of this study is to search for materials that remove high doses of medication in patients, through the quantitative evaluation of the values obtained by the parameters mentioned above.

By presenting a fragile base and ionizes at pH 1.2, diazepam (DZP) is a candidate for study compounds, as it is part of the group of drugs that help to relieve blood pressure and nervousness and other symptoms by reducing the activity of the central nervous system. Part of benzodiazepines that have a similar molecular structure, but differ in functional groups, water solubility and degree of substitution. The hydroxyl groups present in the activated carbon possibly interact with the carbonyl group on the seven- membered ring planar [**19,20**].

In a study where 914 deaths from drug use were analyzed, two deaths were attributed to Diazepam. In these deaths, the doses found in the victims were 5 and 19 mg / L in the blood and 13 mg / kg in the liver. Concentrations greater than 1.5 mg / L in the blood can cause poisoning and toxicity. Deaths attributed to Diazepam occur in a few cases, being verified in concentrations above 5 mg / L in the blood [**21-23**]. In deaths caused by the use of alcohol

and Diazepam, concentrations of 11.4 mg / kg were found in the liver, 6.6 mg / L in the urine, 11.7 mg / kg in the kidney, 4.5 mg / L in the bile, 1.3 mg / L in the blood, 2.4 µg / g in the brain [**24**].

The present work compares commercial activated carbon available on the market in different countries according to the thermodynamic properties and physicochemical parameters for the adsorption of Diazepam (DZP) in simulated gastric fluids (SGF), comparing the data with those available in the literature [**25,26**].

Experimental

Activated carbons

All activated carbons are commercially available in the market for application in the medical, pharmaceutical, and biotechnological field: Norit B test Eur (Germany), Panreac (Spain), BDH (England), Merck (Germany), purified ML (Cuba) and not purified M (Cuba). The activated carbon M was supplied by the Plant Production Baracoa Activated Carbon and treated subsequently by acid/base process (ML) [**22-24**]. The particle size of all samples is 100% under 250 µm. All materials but M meet the requirements of USP30 [**27**].

Simulated gastric fluid

The simulated gastric fluid, according to the USP 30-NF 25, was prepared with the active ingredient chlordiazepoxide (CDZ (51 mg/L). Initially, 2 g of NaCl were dissolved in 7 mL concentrated HCl, and added to 1 L with distilled water free of CO_2, adjusting the pH of the solution to 1.2 [**27**]. UV spectra, **Fig. 1**, related to CDZ and DZP and the calibration curve in SGF, were acquired using a UV/VIS spectrophotometer (Ultrospec 2100 pro, Amersham Biosciences). The optical density of all samples was determined with maximum absorbance at λ_{max} = 242, 284, 366 in the zone of Lambert-Beer transmittance. The calibration curve was adjusted using a least-squares quadratic method, R^2>99. Each experiment was performed in triplicate.

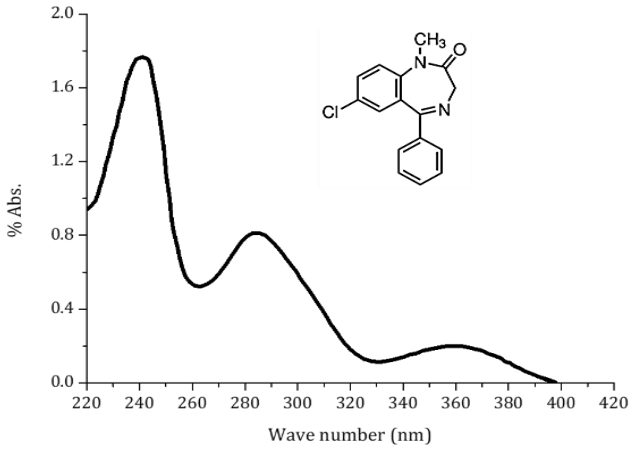

Fig. 1. UV-visible spectrum of DZP.

Batch equilibrium adsorption experiments and analytical method

The particle size distribution of samples of ACs was 100% under 250 µm. During the adsorption process, the amount of carbon used in the range of 0.06 g was added to small vials, 6 mL, previously prepared with the drugs dissolved in SFG. The samples were kept under constant stirring of 150 rpm for 4 h at different temperatures of 300, 306, 310 and 317 K. Then, the samples were filtered to separate the solid phase, and a 5 ml solution was extracted for UV/VIS reading. Experimental solutions at desired concentrations were obtained by diluting the stock solution with SGF adjusted to pH 1.2. Previously established linear Beer-Lambert relationships were used in the concentration analysis. For the solutions with higher concentrations, dilution was required to operate the analysis in the Beer-Lambert region. Absorbance readings were taken from the calibration curve, which determines the equilibrium concentration corresponding to each of the points of the isotherm. The amount of adsorption at equilibrium, q_e (mg/g), was calculated by Eq. (1):

$$q_e = \frac{(C_0 - C_e)V}{M} \quad (1)$$

where, C_0 [mg/mL] is the initial concentration [t = 0] and C_e [mg/ mL], the concentration at equilibrium [t = 4 h], V[L] is the volume of the solution, and M[g] is the weight of carbon.

Adsorption isotherms models

An equilibrium isotherm expresses the relation between the amounts of adsorbate removed from solution at equilibrium by a unit of mass of adsorbent at a constant temperature. Equilibrium data of the Diazepam adsorption were processing by eight "two-parameter isotherms" including Langmuir Tipo I and II, Freundlich, Dubinin-Radushkevich (DR), Temkin, BET, Halsey, and Harkins-Jura [**14-20**]. The linear expressions of those isotherm equations and the way to obtain the isotherm parameters are given in **Table 1**. The least-squares method was used for obtaining the trend lines, and the characteristic parameters were determined from the respective linear form. The best fit among the isotherm models is assessed by the linear coefficient of determination (R^2). In the case of non-linear fitted isotherms, the experimental data and the models calculated were recorded for the higher R^2 value. The lower root means square error (RMSE) test, which measures the difference between the experimental and model data, was considered, too. The mathematical form of this statistic test can be expressed as Eq. (2):

$$RMSE = \sqrt{\left(\frac{1}{n-p}\right)\sum_{1}^{n}\left(q_{e,exp} - q_{e,calc}\right)^2} \quad (2)$$

where, n is the number of data points; p, number of model's parameters, q_{eexp}, experimental adsorption values (mg/g); $q_{e\ calc}$., calculated adsorption values (mg/g).

Table 1. Isotherms and their linearized expressions.

Isotherms	Non-linear models	Linear models	plots
Langmuir	$q_e = q_m\left[\frac{K_L C_e}{1+K_L C_e}\right]$ $\Delta G = -RT\ln[K_L]$	TI $C_e/q_e = \left[\frac{1}{K_{LI}q_m}\right]+\left[\frac{C_e}{q_m}\right]$ TII $\frac{1}{q_e} = \left[\frac{1}{K_{LII}q_m}\right]\left[\frac{1}{C_e}\right]+\frac{1}{q_m}$	$\frac{C_e}{q_e}$ vs C_e $\frac{1}{q_e}$ vs $\frac{1}{C_e}$
Freundlich	$q_e = K_F C_e^{1/n}$	$\ln q_e = \ln K_F + n^{-1}\ln C_e$	$\ln q_e$ vs $\ln C_e$
D-R	$q_e = q_{max}\exp^{-D\varepsilon^2}$ $\varepsilon = RT\ln\left[1+\left(\frac{1}{C_e}\right)\right]$	$\ln q_e = \ln q_{max} - D\varepsilon^2$ $E = [2D]^{-0.5}$	$\ln q_e$ vs ε^2
Temkin	$q_e = \frac{RT}{b}\ln[K_{TK}C_e]$	$q_e = B\ln K_{TK} + B\ln C_e$ $B = \frac{RT}{b}$	q_e vs $\ln C_e$
BET	$q_e = \frac{\left(\frac{C_e}{C_0 - C_e}\right)}{\frac{1}{Kq_m}+\left(\frac{K-1}{Kq_m}\right)*\frac{C_e}{C_0}}$	$\frac{C_e}{q_e(C_0-C_e)} = \frac{1}{q_m K}+\frac{K}{q_m C_e}$	$\frac{\left(\frac{C_e}{C_0-C_e}\right)}{q_e}$ vs $\frac{C_e}{C_0}$
Harkins-Jura	$q_e = \left[\frac{A}{B-\log C_e}\right]^{1/2}$	$\frac{1}{q_e^2} = \frac{B}{A} - \frac{\log C_e}{A}$	$\frac{1}{q_e^2}$ vs $\log C_e$
Halsey	$q_e = \exp^{\left(\frac{\ln K_H - \ln C_e}{n}\right)}$	$\ln q_e = \frac{1}{n}\ln K_H - \frac{1}{n}\ln C_e$	$\ln q_e$ vs $\ln C_e$

Textural characterization

Nitrogen adsorption isotherms of N_2 at 77 K were obtained on a surface analyzer system (Quantachrome Autosorb). The Brunauer, Emmett, Teller (BET), Eq. (3), is the most usual standard procedure used when characterizing an activated carbon. The relative pressure $\left(\frac{P}{P_0}\right)$ range is recommended to obtain the best straight line that is in the range of relative pressures of 0.05 to 0.3. For determining the characteristic BET parameters, it is necessary to plot $\left(\frac{P}{P_0}\right)$ *vs.* $\frac{\left(\frac{P}{P_0}\right)}{V_0\left(1-\frac{P}{P_0}\right)}$, where P (mm Hg) is the applied pressure; P_o (mmHg), the vapor pressure of N_2 at 77 K; V_o (cm^3/g), the volume of adsorbed gas V_m (cm^3), the volume of gas adsorbed monolayer; and C, a constant: [**30**]

$$\frac{\left(\frac{P}{P_0}\right)}{V_0\left(1-\frac{P}{P_0}\right)} = \frac{1}{(V_m C)} + \frac{C-1}{V_m C}\left(\frac{P}{P_0}\right) \quad (3)$$

FTIR

FTIR spectra for the activated carbon samples (4000–400 cm^{-1}) were recorded on an FTIR spectrophotometer (Nicolet 50X). The samples were prepared with KBr pellets containing 0.1 wt % carbon, which were dried for 12 h at 100°C before the spectra were recorded.

Thermodynamic parameters of adsorption

The change in Gibbs free energy of the sorption process is related to the sorption equilibrium constant, K_{ads}, by the classical Van`t Hoff equation, Eq. (9):[**13,14,28,29**].

$$\Delta G^0_{ads} = -RT\ln K_{ads} \quad (4)$$

Since $\Delta G^0_{ads} = \Delta H^0 - T\Delta S^0$, K_{ads} is obtained from the following relationships using the experimental data, Eq. (9-12):

$$ln\, K_{ads} = -\frac{\Delta H^0}{RT} + \frac{\Delta S^0}{R} \quad (5)$$

$$K_{ads} = \left[\left(\frac{C_0 - C_e}{C_e}\right)\right]\left[\frac{V\rho}{w}\right] = \frac{q_e \rho}{C_e} \quad (6)$$

$$ln\left[\frac{q_e}{C_e}\right] = -\frac{\Delta H^0}{RT} + \frac{\Delta S^0}{R} \quad (7)$$

where ρ is the density of the solution (g/L); ΔG^0, the free energy change (kJ/mol); ΔH^0, the standard enthalpy change (kJ/mol); T, the absolute temperature (K); K_{ads}, the equilibrium constant of interaction between the adsorbate and the ACs surface; R, the universal gas constant (8.31 J/mol K); ΔS^0, the entropy of the system. ΔH^0 can thus be determined from the slope of the Van`t Hoff plot ln (q_e/C_e) vs 1/T and the intercept represent the entropy variation ΔS^0.

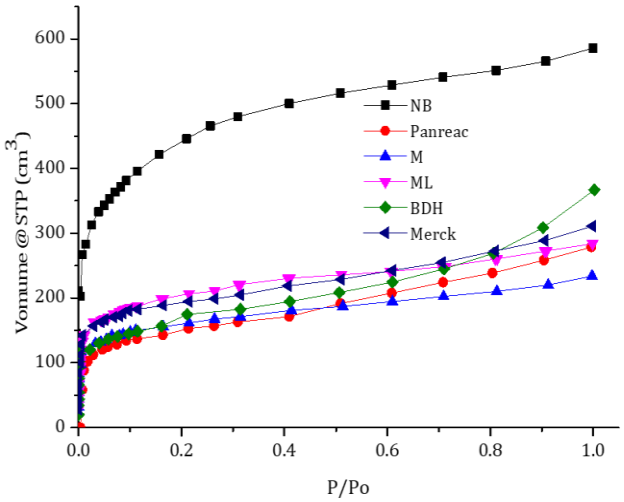

Fig. 2. N_2 adsorption isotherms at T = 77 K: ML, BDH, Merck, M, Panreac, NB.

Results and discussion

Specific surface area determination and volume distribution of activated carbon

The N_2 adsorption isotherms at 77 K are shown in **Fig. 2**. The values obtained after evaluating the BET Equation in its linear form are reported in **Table 2**. Surface areas are in a normal range for this type of material. Three groups of surface areas can be distinguished corresponding to a very high surface area of 1400m^2/g (NB), the second one value of the surface area of 720m^2 /g (ML), and the third one group around 550 m^2/g (M and Panreac, Merck, BDH). Concerning surface area ratios established between these materials, and the value of the surface area of NB, the following increasing order was observed:1 (NB), 1.98 (ML)), 2.63 (BDH), 2.65 (M, Panreac), respectively. Among ML and M, there is a difference between their surface areas of 102 m^2/g, due to the chemical modification in the case of ML [**19,20,25**]. Much of the inorganic material initially present in M was removed during the acid leaching for exposing the obstructed porosity, which reached 34%. These new unlocked pores allow access of the N_2 molecule (16.2 A^2 and 0.3 nm), thus contributing to further development of the internal surface area of ML, which achieved 1.34 times the internal surface area of untreated M.

Table 2: Surface area of activated carbons and volume of monolayer N_2 at 77 K obtained from BET Equation.

Adsorbent	Surface area (m^2/g)	Monolayer volume (cm^3/g)
Norit B	1430	328
ML	721	165
M	539	123
Merck	614	141
BDH	543	125
Panreac	539	123

The surface area is simply the result of the entire area occupied by nanopores, once the molecule is introduced into these N_2 to fill the volume corresponding to a monolayer (V_m), **Table 2**. The pore size distribution was calculated by different methods: DFT (density functional theory), HK (Howart-Kawasoe) and MP (micropore method), **Table 3**. The calculation of micropores (0.3 to 2 nm) from the adsorption isotherm of CO_2 at 273 K reveals no substantial differences in comparison to those values calculated from the isotherm of N_2, which is indicative that these materials are predominantly microporous. They do not fail to show the development of narrow mesopores (2 to 3 nm), **Fig. 3**. However, it is precisely in this zone where most of these materials show very similar textural development. Except for NB, it was further noted that for M and ML, in the area corresponding to pores with sizes between 2.3 to 3 nm, an increase in the volume of mesopores was due mainly to ML's chemical cleaning.

Between 0.5 to 1 nm, a significant increase was found in the volume of micropores in ML, caused by the same reasons. Starting from 2 nm, the rest of the activated carbons presented definite trends in the development of micropore volume with significant variation between them, due to their fabrication process and raw materials.

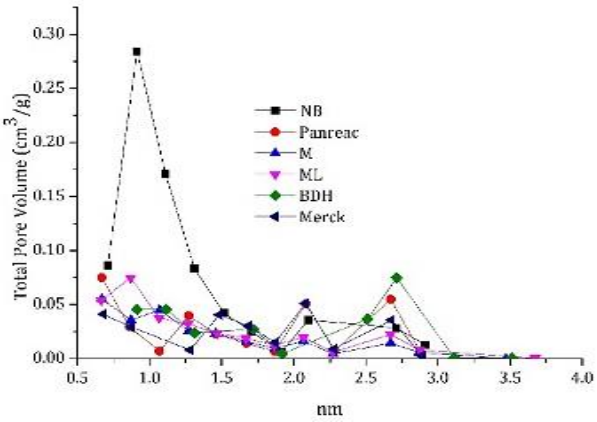

Fig. 3. Distribution of pores (MP method) by N_2 adsorption at 77 K: ML, BDH, Merck, M, Panreac, NB.

Table 3. Total pores volume and average pore size obtained from different methods: DFT: density functional theory[1], HK: Howart-Kawasoe[2] and MP: Micropores[3].

Adsorbent	DFT (cm^3/g)	HK (cm^3/g)	MP (cm^3/g)
NB	0.81	0.65	0.77
ML	0.40	0.30	0.31
M	0.33	0.26	0.24
Merck	0.42	0.31	0.24
BDH	0.35	0.23	0.29
Panreac	0.39	0.23	0.26

Identification of surface functional groups

To verify the details of the functional groups at the surface of the activated carbon samples, FTIR spectra were determined. In **Table 4**, the bands and the variation of the

relative chemical species for each AC type can be observed with more details and the identification of the main present functional group**s.** A percentile distribution of the functional groups found in the group of the samples of AC follows: 100% for the bands of 3500-3400 cm^{-1} and 2800-3000 cm^{-1}, respectively, 75% for 1460, 1125 and 950 cm^{-1}, a 63% (1730, 1600-1650 cm^{-1}), 50% (1631, 1581-1585 cm^{-1}), 38% (1635, 1435, 1100-1200 cm^{-1}) and 25% (1730-1720, 1710 cm^{-1})[29–34].

A typical example is the adsorption of hydrophobic molecules onto hydrophobic adsorbents from diluted aqueous solutions that can present an absolute repulsion to the water and present good AC surface attraction. The AC surface is loaded positively because of the values pH_{zpc}<pH = 1.2, which is favorable for the possibility of dissociation of Diazepam.

Table 4. Characteristic bands and associated functional groups identified by FTIR.

Bands (cm^{-1})	functional groups	Activate carbon					
		NB	Merck	Panreac	BDH	ML	M
3400-3500	OH phenol	x	x	x	x	x	x
2800-3000	C-H, $–CH_2$, $-CH_3$aliphatic	x	x	x	x	x	x
1698	Aryl ketone C=O stretch	x					
1720-1730	C-O carbonyl	x					
1710	C=O can be assigned either to lactone or to nonaromatic carboxyl groups, for which the	x			x		
1600-1650	C=O quinonics groups	x		x	x	x	
1635	N–H			x		x	
1631	C=O stretching of amide	x				x	
1580-1585	C=O aromatic ring stretching couplet of highly conjugated carbonyl groups	x	x		x	x	x
1460	OH, carboxyl groups, and vibration C-H	x	x		x	x	
1440	OH carboxylic						x
1100-1200	C-O phenolic or esters	x		x	x	x	
1125	OH carboxyl	x	x		x	x	x
1040	C-O alcoholic vibration stretching				x		
< 950	C-H aromatic ring vibration		x			x	x

This analysis confirms that the activated carbon ML and M were obtained from the same original material, by the same activation process. In the case of ML, the purification introduced structural alterations in both hydrophobic and hydrophilic planes. In ML, 11 functional groups and were identified, and in M, only 7 of them were detected.

Diazepam adsorption

Diazepam adsorption's experimental data at 310 K and pH = 1.2 are presented in **Fig. 4** and **Table 5**. The Diazepam molecule is a weak base with pKa= 3.5> pH = 1.2, which mainly guarantees its molecular state in the system. However, some molecules may be dissociated by the proximity of these two values. Its solubility as a free base is very low. Besides, the Diazepam molecule, as likely all benzodiazepines, has hydrophobic properties, supporting the strong hydrophobic interactions with the basal plane of AC. Moreover, as discussed in previous works, carbonyl groups' presence are susceptible to interacting with the hydroxyl groups on the AC surface. Thus, these specific interactions could justify the excellent adjustment of the Langmuir equation. It should also clarify that the molecules are absorbed, not only because they can be attracted to the solid surfaces but also because the solution can reject them.

The adjustment of each adsorption isotherm model was evaluated, as shown in **Table 5**. The model that best fits the experimental data is the Langmuir TI. A single model can explain the results obtained for Diazepam adsorption. The obtained results are in accordance with the monolayer formation (specific interactions) and adsorption in the hydrophobic plane.

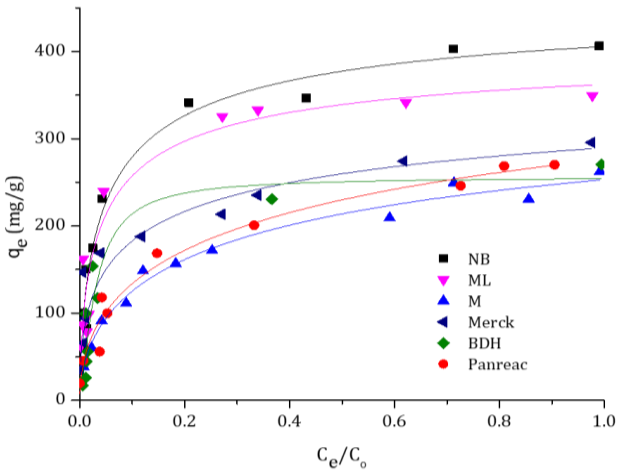

Fig. 4 Experimental data of adsorption isotherms profile of Diazepam in SGF: NB, ML, M, Merck, BDH, Panreac.

Table 5. Characteristic parameters of models for Diazepam adsorption in different activated carbons.

		Activated carbon							
Models	**Parameters**	**ML**	**NB**	**NE**	**Panreac**	**M**	**BDH**	**Merck**	**Average**
DR	D	$1.3x10^{-4}$	$1.2x10^{-4}$	$1.5x10^{-4}$	$1.4x10^{-4}$	$1.6x10^{-4}$	$1.1x10^{-4}$	$1x10^{-4}$	
	E	61.63	63.57	62.08	59.76	60.41	67.42	70.71	
	q_m	1188	1451	1289	1212	963	846	804	
linear model	R^2	0.87	0.93	0.86	0.95	0.94	0.76	0.85	0.87
q_{exp}/q_{calc}	R^2	0.89	0.94	0.90	0.98	0.97	0.89	0.92	0.93
$q_{exp}/q_{calc\ (non\text{-}linear)}$	RAMSE	15	38	53	13	15	37	27	30
LTI	q_m	417	00	472	370	286	278	345	
	K_{LI}	2400	1000	1060	450	500	720	967	
linear model	R^2	0.99	0.99	0.99	0.98	0.98	0.986	0.989	**0.99**
q_{exp}/q_{calc}	R^2	0.93	0.98	0.97	0.91	0.91	0.93	0.93	**0.93**
$q_{exp}/q_{calc\ (non\text{-}linear)}$	RAMSE	62	55	64	163	136	36	57	**89**
LTII	q_m	333	500	333	200	200	206	333	
	K_{LII}	1000	1000	3000	1667	2500	1426	1500	
linear model	R^2	0.85	0.92	0.87	0.95	0.82	0.92	0.91	0.89
q_{exp}/q_{calc}	R^2	0.91	0.98	0.96	0.88	0.76	0.91	0.90	0.91
$q_{exp}/q_{calc\ (non\text{-}linear)}$	RAMSE	275	58	35	82	42	46	53	127
Freundlich	K_F	1755	1636	1536	1366	963	1998	992	
	n	2.94	3.13	2.94	2.48	2.99	2.17	3.47	
linear model	R^2	0.82	0.930	0.856	0.940	0.935	0.762	0.84	0.86
q_{exp}/q_{calc}	R^2	0.88	0.93	0.90	0.55	0.97	0.86	0.92	0.87
$q_{exp}/q_{calc\ (non\text{-}linear)}$	RAMSE	54	39	46	105	14	46	28	60
Hasley (pend -)	K_H	$34.2x10^8$	$11x10^9$	$28.1x10^8$	$66.9x10^6$	$58.1x10^7$	$11.3x10^6$	$68.5x10^7$	
	n	2.94	3.13	2.94	2.48	2.99	2.17	2.94	
linear model	R^2	0.82	0.92	0.86	0.94	0.94	0.76	0.84	0.86
q_{exp}/q_{calc}	R^2	0.85	0.81	0.95	0.72	0.82	0.75	0.91	0.84
$q_{exp}/q_{calc\ (non\text{-}linear)}$	RAMSE	28626	23059	24120	36119	7440	78189	10188	28935
Temkin	K_{TK}	38615	71822	29132	15977	14071	2.7	59515	
	B	57	58	59	44	42	44	40	
	b	45	44	44	59	61		65	
linear model	R^2	0.94	0.96	0.97	0.94	0.94	0.91	0.94	0.94
q_{exp}/q_{calc}	R^2	0.93	0.96	0.97	0.72	0.94	0.91	0.94	0.92
$q_{exp}/q_{calc\ (non\text{-}linear)}$	RAMSE	36	43	23	89	19	30	22	35
H-J	A	12500	12500	8333	1818	5555	909	14286	
	F	2	1.25	2.1	2.25	1.94	2.42	1.86	
linear model	R^2	0.70	0.69	0.41	0.44	0.61	0.38	0.57	0.51
q_{exp}/q_{calc}	R^2	0.91	0.96	0.95	0.31	0.96	0.91	0.93	0.86
$q_{exp}/q_{calc\ (non\text{-}linear)}$	RAMSE	194	224	205	169	149	159	141	174
BET	q_m	15	141	29	37	43	20	24	
	A	11	71	35	27	23	15	21	
linear model	R^2	0.66	0.93	0.75	0.79	0.79	0.52	0.73	0.73
q_{exp}/q_{calc}	R^2	0.64	0.71	0.69	0.12	0.87	0.30	0.76	0.59
$q_{exp}/q_{calc\ (non\text{-}linear)}$	RAMSE	264	278	263	190	194	183	207	21

Regarding the Diazepam molecule's size, it is not a barrier to transport by diffusion through the micropores of AC. The Diazepam molecule diameter is about 8.3 Å, and this size requires to avoid steric effects during diffusion through the pores should range between 1.2 - 1.7 of the diameter adsorbed molecule, which corresponds to 9.96 - 14.11 Å pore diameters of the AC. Pores did not find the access limitation in this respect for all AC and pore size sufficient to adsorb the Diazepam molecule.

To get a better understanding of the textural parameters defining the Diazepam sorption behavior at adsorption condition, **Fig. 5** shows the evolution of adsorption capacity (mg/g) for all activated carbons as a function of the surface area and total pore volume. Curves were drawn showing the dependence of Diazepam adsorption value: on the specific surface (**Fig. 5(a)**) and total pore volume calculated by different methods: DFT (**Fig. 5(b)**), HK (**Fig. 5(c)**), and MP method (**Fig. 5(d)**). The values of coefficients were determined to describe the dependence of structural parameters. The best correlation between Diazepam adsorption was obtained for the surface area- $R^2 = 0.86$. It is worth noting that the R^2 values for the correlation between Diazepam adsorption and the total volume of pores, obtained by various methods (DFT, HK, MP), were similar- $R^2 = 0.78 \pm 2$. On this basis, it can be concluded that the value of Diazepam adsorption for all tested activated carbons was dependent on the surface area.

Thermodynamics properties

The thermodynamic properties analyzed are shown in Table 4 and **Fig. 6** and **Fig. 7**. In all cases, it is observed that the adsorption enthalpies are positive for DZP. That indicates that the adsorption is endothermic. The ΔH values' magnitude lies in the range of 2.1 to 20.9 and 80 to 200 kJ/mol for physical and chemical adsorption, respectively [**35,36**]. Enthalpy of adsorption

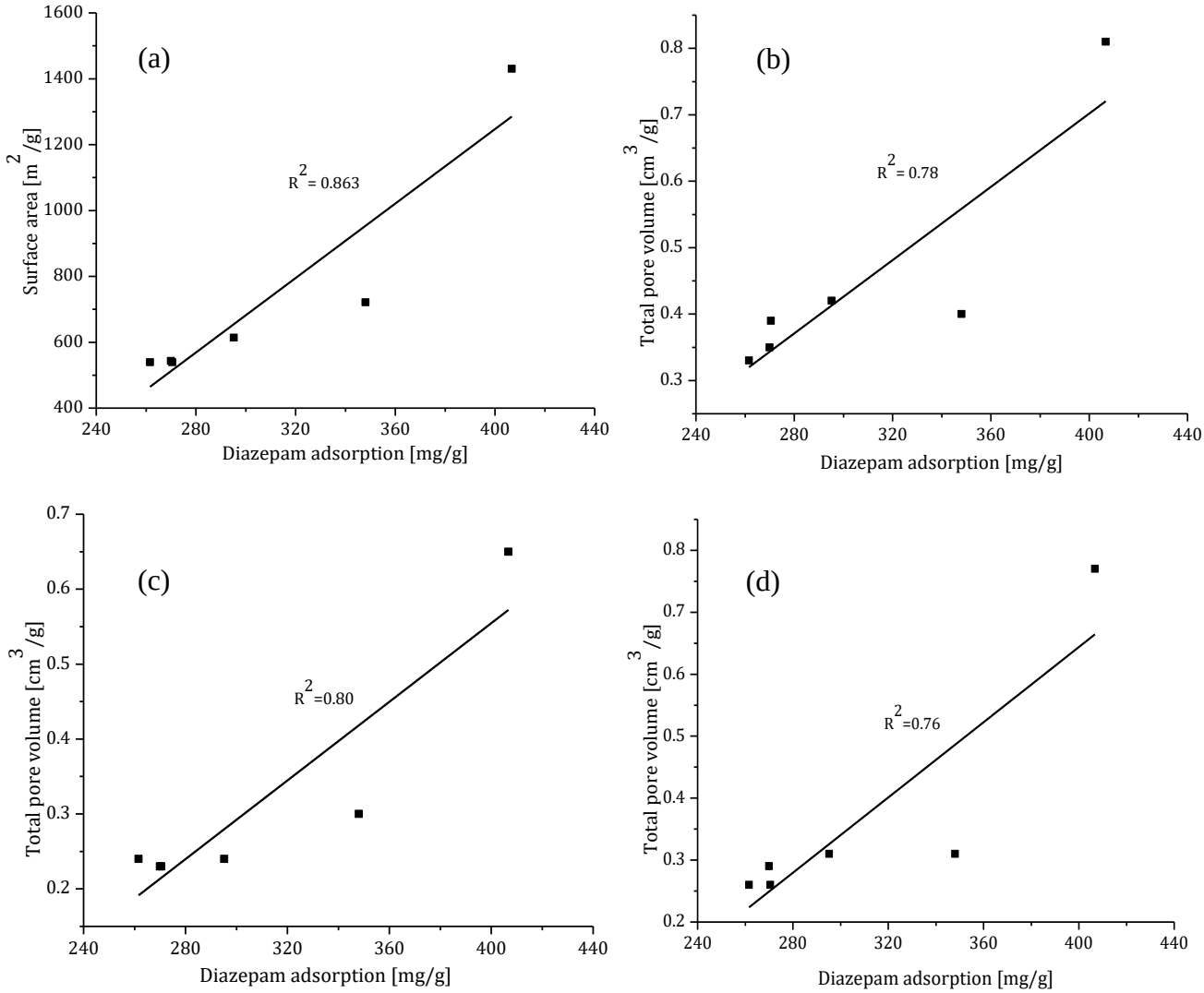

Fig 5. Correlation between the Diazepam adsorption as a function of surface area (a), and total pore volume calculated by: DFT (b), HK (c), and MP method (d).

was found to be in the range of 9.83 to 67.44 kJ/mol. The enthalpy values obtained for the case of DPZ are less than 80 kJ/mol, but in the majority of cases more significant than 20 kJ/mol, except for BDH and Merck. This indicates that DPZ needs to involve lower energy for adsorption due to the specific interaction characteristics of the system.

Generally, ΔG is in the range of 0 to -20 kJ/mol and -80 to - 400 kJ/mol for physical and chemical adsorption [**37-40**]. The values of ΔG^0 calculated are in the range of physical adsorption, **Table 6**. The positive values of ΔS^0, Table 4, decreased randomness at the solid/solution interface, and within the degree of freedom of the adsorbed species. The value of ΔG is found to be in the range of -16.60 to -18.18 kJ/mol for the whole studied temperature range. The negative value of ΔG indicates the feasibility and spontaneity of the adsorption process in both cases [**38-40**].

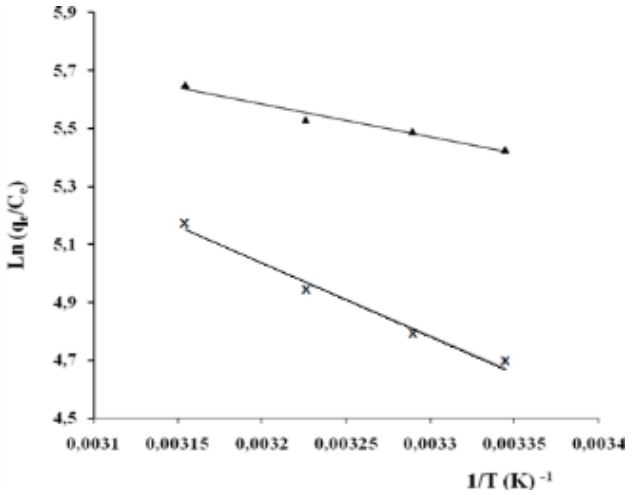

Fig. 6. Van`t Hoff plot of adsorption (ΔH_{ads}< 20 kJ/mol) equilibrium constant K_{ads} for adsorption of DZP (ΔH< 20 kJ/mol) onto BDH (x), Merk (♦).

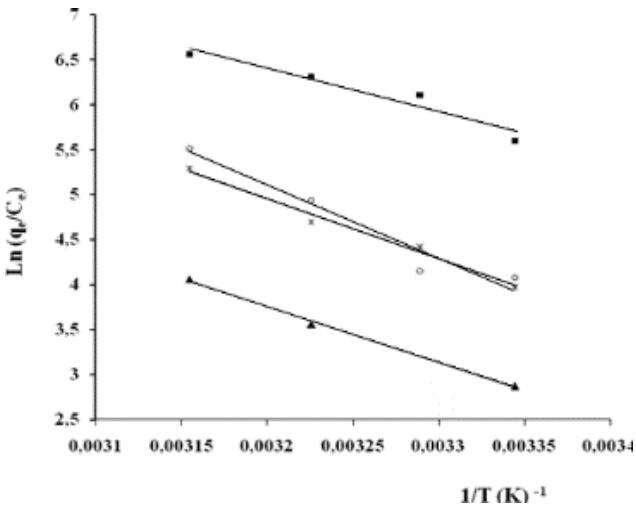

Fig. 7. Van`t Hoff plot of adsorption (ΔH_{ads}> 20 kJ/mol) equilibrium constant K_{ads} for adsorption of DZP onto NB (o), ML (■), M (▲), Panreac (*).

Table 6. Thermodynamic parameters for the adsorption of DZP onto ACs in SGF.

Adsorbate	Thermodynamic parameters				
	ΔH^0 (kJ/mol)	ΔS^0 (J/mol)	$T\Delta S^0$ (K) (J/mol)	ΔG^0 (kJ/mol)	R^2
NB	67.44	260	77.03	-10.13	
			78.31	-10.50	0.977
			79.86	-12.72	
			81.66	-14.53	
ML	55.39	220	65.30	-9.88	0.986
			66.39	-11.16	
			67.70	-12.10	
			69.23	-13.94	
M	51.84	200	58.89	-7.13	0.997
			59.87	-9.86	
			61.05	-9.18	
			62.43	-10.70	
BDH	20.87	110	32.55	-11.67	0.990
			33.09	-11.98	
			33.75	-12.84	
			34.51	-13.63	
Merck	9.83	80	23.31	-13.48	0.964
			23.70	-13.87	
			24.16	-13.88	
			24.71	-14.89	
Panreac	40.16	180	54.34	-13.91	
			55.25	-15.42	0.973
			56.34	-16.26	
			57.61	-17.29	

Conclusions

Activated carbons showed high adsorption capacity for Diazepam. The results showed that the adsorption capacity of Diazepam is dependent on the specific surface area of ACs (R^2 = 0.86). The best linear (R^2 = 0.99) and non-linear (R^2 = 0.93, RAMSE = 83) fittings of isotherms models were obtained with Langmuir TI, which assumes monolayer adsorption and specific interactions of Diazepam in FGS and was found to be applicable for ACs. The thermodynamic values in the adsorption process are characterized by ΔH > 0, ΔG < 0 and ΔS> 0. The positive values of all the isosteric adsorption enthalpies for both drugs indicate the endothermic nature of adsorption, and the decrease of the free Gibbs energy (ΔG) with the increase of temperature. Isosteric enthalpy of adsorption was found to be in the range of 9.83 to 67.44 kJ/mol which are considered low values. The enthalpy values obtained are less than 80 kJ/mol but in most cases greater than 20 kJ/mol, except for BDH (20.87 kJ/mol) and Merck (9.83 kJ/mol),

respectively. The values of ΔG were negative in all cases, which confirms the spontaneous character of the adsorption process. The positive value of ΔS^0 decreased randomly at the solid/solution interface with some structural change in the adsorbate and adsorbent, and the entropy change increased with the increase of substitution degree. Due to the adsorption capacity of these materials, their application as an antidote for Diazepam is suggested.

Acknowledgements

The authors express their appreciation to Programa de Estudantes-Convênio de Pós-Graduação (PEC/PG), Coordenação de Aperfeiçoamento de Pessoal de Nível Superior (Capes) and Fundação de Amparo à Pesquisa do Estado do Amazonas (FAPEAM), in Brazil. The authors would also like to thank the helpful cooperation with MEDSOL Laboratories, Reinaldo Gutierrez Laboratories and Bioinorganic Department from Universidad de la Habana, in Cuba.

Keywords

Activated carbon, adsorption of drugs, thermodynamics parameters, diazepam, isotherms.

Received: 6 November 2020
Revised: 22 January 2021
Accepted: 13 February 2021

References

1. *J. Toxicol. Clin. Toxicol.*, **1999**, *37*, 731.
2. Chyka, P. A.; Seger, D.; Krenzelok, E. P.; Vale, J. A.; *Clin. Toxicol. (Phila).*, **2005**, *43*, 61.
3. Neuvonen, P. J.; Olkkola, K. T.; *Med. Toxicol. Adverse Drug Exp.* **1988**, *3*, 33.
4. Alaspää, A. O.; Kuisma, M. J.; Hoppu, K.; Neuvonen, P. J.; *Ann. Emerg. Med.*, **2005**, *45*, 207.
5. Terzyk, A. P.; *J. Colloid Interface Sci.*, **2002**, *247*, 507.
6. Terzyk, A. P.; Rychlicki, G.; Biniak, S.; J. P. Łukaszewicz, *J. Colloid Interface Sci.*, **2003**, *257*, 13.
7. Moreno-Castilla, C.; *Carbon N. Y.*, **2004**, *42*, 83.
8. Pradhan, B. K.; Sandle, N. K.; *Carbon N. Y.*, **1999**, *37*, 1323.
9. Smisek, M.; Cerny, S.; *Anal. Chem.*, **1970**, *42*, 81A.
10. VanDer Kamp, K. A.; Qiang, D.; Aburub, A.; Wurster, D. E.; *Langmuir*, **2005**, *21*, 217.
11. Aburub, A.; Wurster, D. E.; *J. Colloid Interface Sci.*, **2006**, *296*, 79.
12. Burke, G. M.; Wurster, D. E.; Berg, M. J.; Veng-Pedersen, P.; Schottelius, D. D., *Pharm. Res.*, **1992**, *9*, 126.
13. Kumar, A.; Prasad, B.; Mishra, I. M.; *J. Hazard. Mater.*, **2010**, *176*, 774.
14. Kumar, A.; Prasad, B.; Mishra, I. M.; *J. Hazard. Mater.*, **2008**, *152*, 589.
15. Behnamfard, A.; Salarirad, M. M.; *J. Hazard. Mater.*, **2009**, *170*, 127.
16. Richard, D.; M. de L. Delgado Núñez; Schweich, D.; *Chem. Eng. J.*, **2009**, *148*, 1.
17. Xin, X.; Si, W.; Yao, Z.; Feng, R.; Du, B.; Yan, L.; Wei, Q.; *J. Colloid Interface Sci.*, **2011**, *359*, 499.
18. Ahmad, M. A.; Rahman, N. K.; *Chem. Eng. J.*, **2011**, *170*, 154.
19. Wurster, D. E.; Alkhamis, K. A.; Matheson, L. E.; *J. Pharm. Sci.*, **2003**, *92*, 2008.
20. Hussein, H. K. A.; *Iraqi J. Pharm. Sci.*, **2005**, *14*, 36.
21. Moheni, H.; in Int. Assoc. Forensic Toxicol., **1975**.
22. de Silva, J. A. F.; Munno, N.; D'Arconte, L.; Strojny, N.; *J. Pharm. Sci.*, **1978**, *67*, 752.
23. Finkle, B. S.; *JAMA*, **1979**, *242*, 429.
24. Simon, R. K.; in Int. Assoc. Forensic Toxicol., **1976**.
25. J. C. L. A. I. *. Carlos A. Rey Mafull, *Rev. CENIC Ciencias Químicas.*, **2006**, *38*, 1.
26. Rey-mafull, C. A.; Iglesias-cerveto, A.; Aja-muñiz, R. G. R.; *Rev. CENIC Ciencias Químicas.*, **2010**, *41*, 167.
27. United States Pharmacop, **2007**.
28. Kubilay, Ş.; Gürkan, R.; Savran, A.; Şahan, T.; *Adsorption*, **2007**, *13*, 41.
29. Moreno-Castilla, C.; López-Ramón, M.; Carrasco-Marín, F.; *Carbon N. Y.*, **2000**, *38*, 1995.
30. Yang, T.; Lua, A. C.; *J. Colloid Interface Sci.*, **2003**, *267*, 408.
31. Puziy, A.; Poddubnaya, O.; Martínez-Alonso, A.; Suárez-García, F.; Tascón, J. M.; *Carbon N. Y.*, **2003**, *41*, 1181.
32. El-Sharkawy, E. A.; Soliman, A. Y.; Al-Amer, K. M.; *J. Colloid Interface Sci.*, **2007**, *310*, 498.
33. Valix, M.; Cheung, W. H.; McKay, G.; *Langmuir*, **2006**, *22*, 4574.
34. Chen, X.; Farber, M.; Gao, Y.; Kulaots, I.; Suuberg, E. M.; Hurt, R. H.; *Carbon N. Y.*, **2003**, *41*, 1489.
35. Shin, S.; Jang, J.; Yoon, S.H.; Mochida, I.; *Carbon N. Y.*, **1997**, *35*, 1739.
36. Mall, I. D.; Srivastava, V. C.; Agarwal, N. K.; Mishra, I. M.; *Chemosphere*, **2005**, *61*, 492.
37. Liu, Y.; *J. Chem. Eng. Data*, **2009**, *54*, 1981.
38. Li, Y.H.; Di, Z.; Ding, J.; Wu, D.; Luan, Z.; Zhu, Y.; *Water Res.*, **2005**, *39*, 605.
39. Liu, Q.S.; Zheng, T.; Wang, P.; Jiang, J.P.; Li, N.; *Chem. Eng. J.*, **2010**, *157*, 348.
40. Hameed, B. H.; *Colloids Surfaces A Physicochem. Eng. Asp*, **2007**, *307*, 45.